

1 *Supporting Information for*  
2 Sensitivity of urban heat islands to various  
3 methodological schemes

4 Gemechu Fanta Garuma <sup>\*1</sup>

<sup>1</sup> *Entoto Observatory and Research Center (EORC), Atmospheric and Climate (AtClim) Sciences Unit, Department of Space and Planetary Sciences at the Space Science and Geospatial Institute (SSGI), Addis Ababa, Ethiopia.*

5  
6 **Contents of this file**

- 7  
8 a. Table S1  
9 b. Figures S1 to S7

Seasons	Mean daytime TSUHI values			
	Method 1 (M1)	Method 2 (M2)	Method 3 (M3)	Mean(M1,M2,M3)
Summer	0.72°C	1.03°C	0.74°C	0.83°C
Autumn	0.92°C	1.29°C	0.30°C	0.84°C
Winter	-0.29°C	-0.28°C	0.89°C	0.11°C
Spring	-0.87°C	-0.97°C	-0.58°C	-0.81°C

Seasons	Mean nighttime TSUHI values			
	Method 1 (M1)	Method 2 (M2)	Method 3 (M3)	Mean(M1,M2,M3)
Summer	0.22°C	0.33°C	0.30°C	0.28°C
Autumn	0.53°C	0.76°C	0.30°C	0.53°C
Winter	0.81°C	1.07°C	0.89°C	0.92°C
Spring	0.56°C	0.78°C	-0.58°C	0.25°C

Table S1: This table shows the different mean TSUHI values for each of the methods, M1, M2, and M3. The observation TSUHI estimation and the mean of the methods, Mean(M1,M2,M3) are also shown for comparison.

---

\***Corresponding author:** Gemechu Fanta Garuma, Research Scientist and Assistant Professor, email: gemechuf@essti.gov.et & gemechufanta@gmail.com

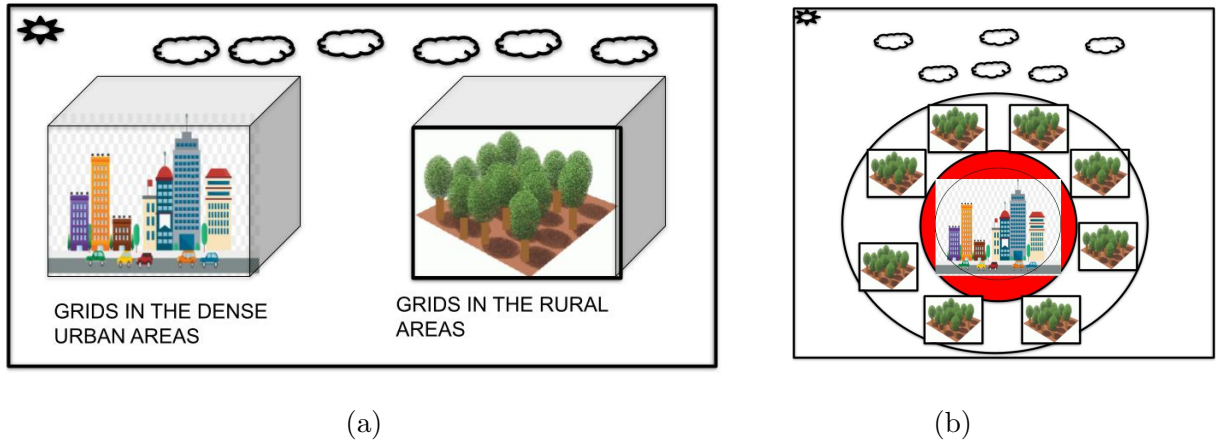


Figure S1: The figure depicts two common approaches to representing urban and rural areas in urban climate studies: (a) separate grids for urban and rural regions, (b) urban area at the center surrounded by rural grid cells.

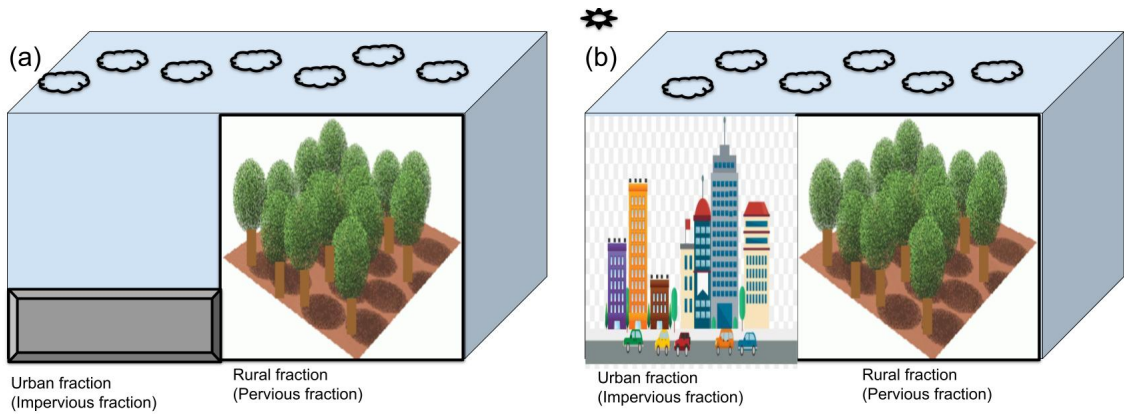


Figure S2: The figure compares two approaches to incorporating urban features into a combined urban-rural grid: (a) a simplified model with adjustments for impervious surfaces like pavement, and (b) a more detailed representation including buildings, roads, and other impervious elements.

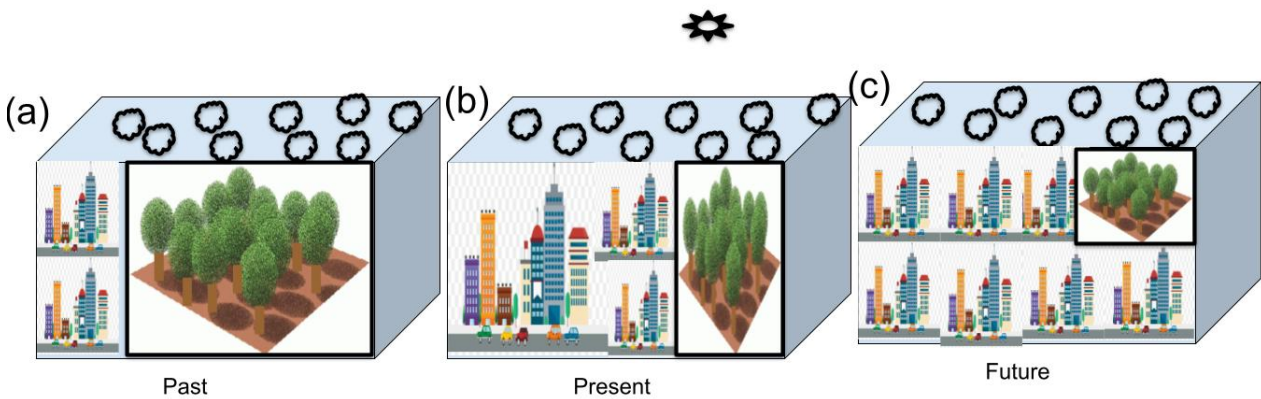


Figure S3: A diagrammatic representation of the hypothetical urban and rural grids in the (a) past (b) present and (c) future. The rural grids decrease from the past to the future as more urban areas are expected to replace most of the natural fractions.

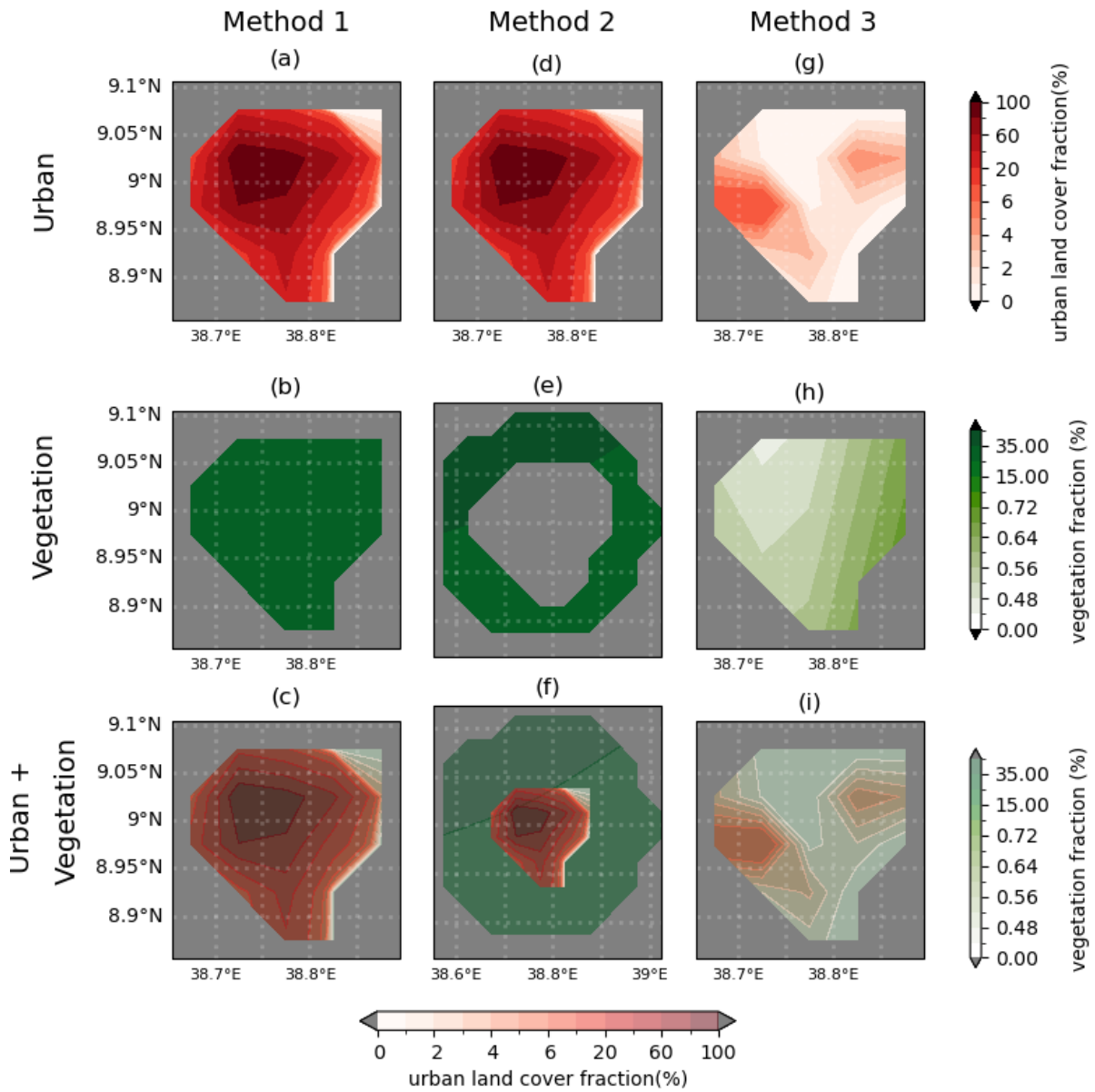


Figure S4: Three frequently used methods to quantify urban and rural properties, Method 1: Urban land cover fractions (a) and vegetation fractions (b) are used to differentiate urban and rural areas, whereas the combined urban and vegetation fractions are shown in (c), Method 2: urban at center (d) and rural areas surrounding it (e) are used to quantify urban and rural properties, whereas the combined Urban and vegetation fractions are shown in (f), and Method 3: Urban dynamics: the differences between urban land cover (g) and vegetation fraction (h) in the first few years (2000-2010) when urban development was low and the next few years (2011-2020) after the city had gone through huge urban development, whereas the combined urban and vegetation dynamics is shown in (i).

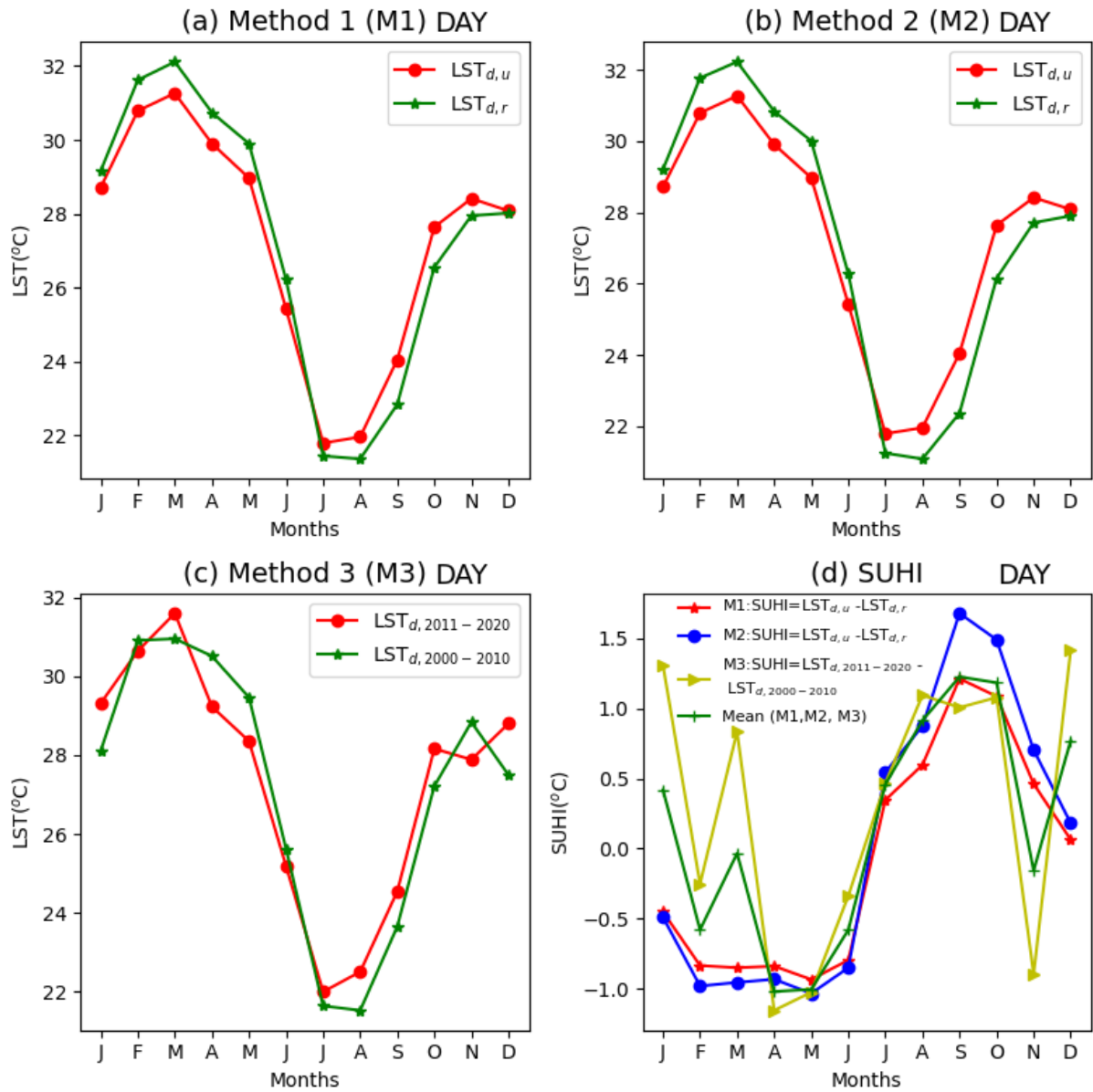


Figure S5: The different methods, (a) method 1, (b) method 2 and (c) method 3, to compute the urban and rural land surface temperature annual cycles. The tropical surface urban heat islands shown in (d) are calculated based on these methods and compared with TSUHI computed from the ground based observation.

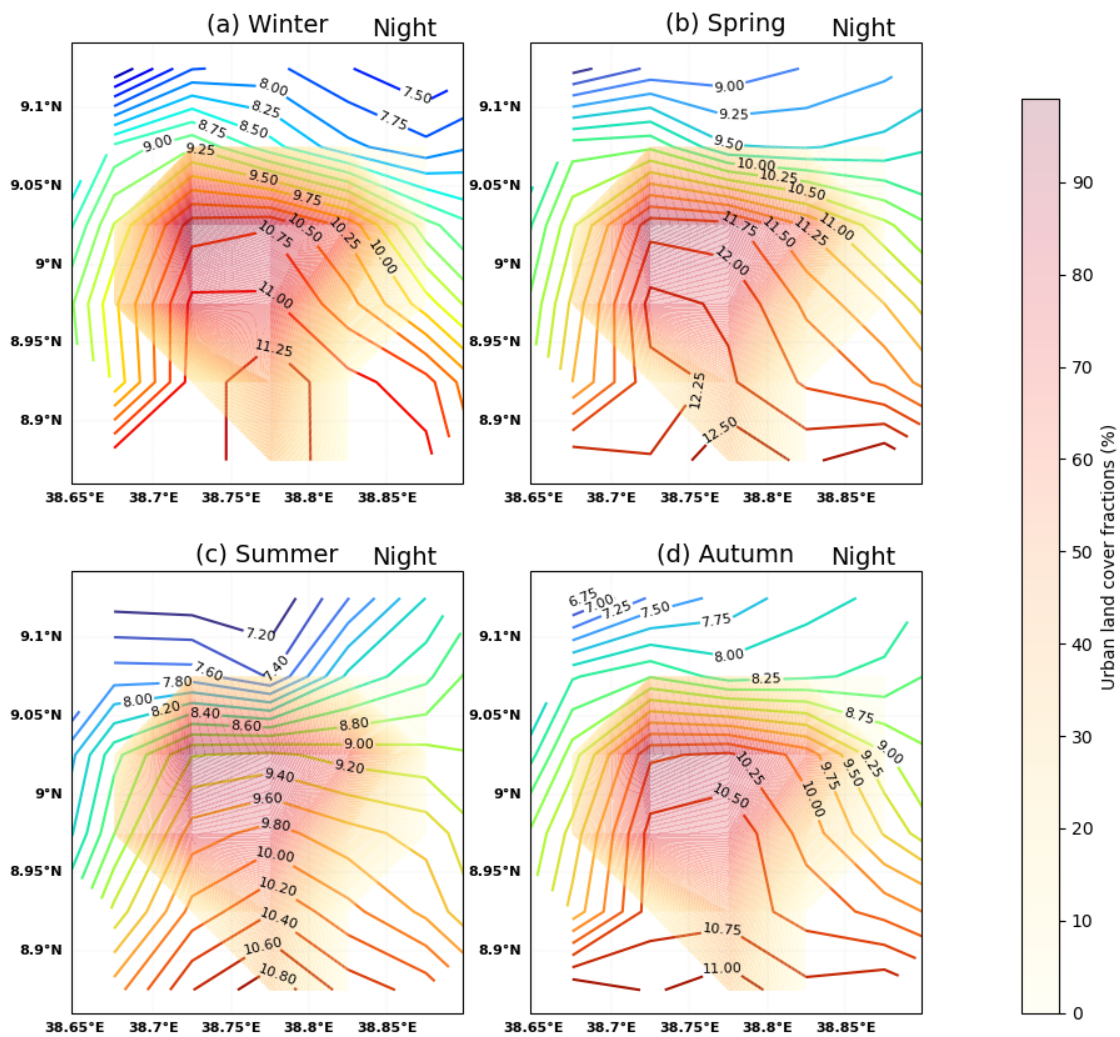


Figure S6: Seasonal mean (2000-2020) MODIS represented land surface temperature contour lines for (a) winter, (b) spring, (c) summer, and (d) autumn seasons during the night time.

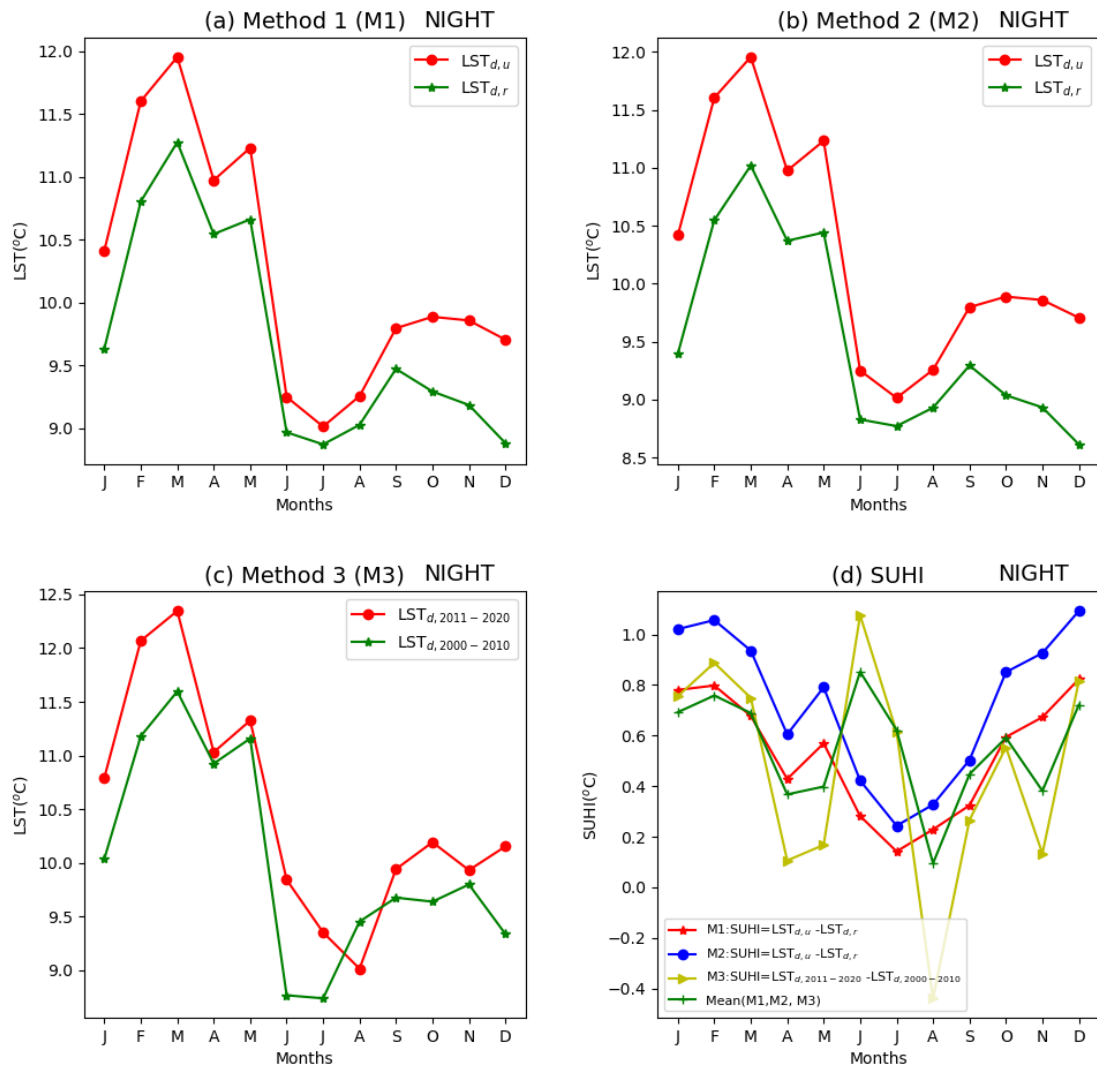


Figure S7: The different methods, (a) method 1, (b) method 2 and (c) method 3, to compute the urban and rural land surface temperature annual cycles during the night. The corresponding nighttime tropical surface urban heat islands are shown in (d).